

Two New Iron(II) Spin-Crossover Complexes with N_4O_2 Coordination Sphere and Spin Transition around Room Temperature

Birgit Weber,^{*[a]} Jaroslava Obel,^[a] Dunie Henner-Vásquez,^[a] and Wolfgang Bauer^[a]

Keywords: Iron / Magnetic properties / Spin crossover / Schiff bases

The reaction of iron(II) acetate with the tetradentate Schiff base like ligand H_2L1 {[3,3']-[4,5-dihydroxy-1,2-phenylene-bis(iminomethylidene)bis(2,4-pentanedion)]} leads to the formation of the complex $[FeL1(MeOH)]$. Reaction of this complex with pyridine (py) or *N,N'*-dimethylaminopyridine (dmap) leads to the two N_4O_2 -coordinated complexes $[FeL1(py)_2] \cdot py$ (**1**) and $[FeL1(dmap)_2] \cdot MeOH \cdot 0.5dmap$ (**2**). Both complexes are spin-crossover compounds that were characterised by using magnetic measurements, X-ray crystallography and temperature-dependent 1H NMR spectroscopy. Special attention was given to the role of the two

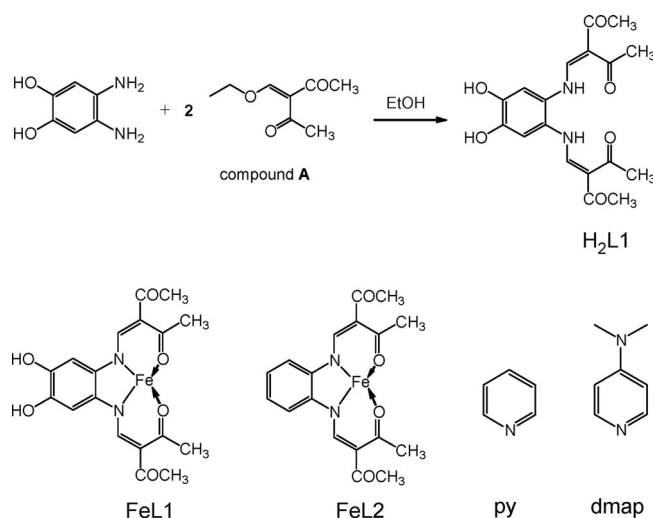
hydroxy groups on the phenyl ring in the formation of a hydrogen-bonding network and the influence of this network on the spin-transition properties. Although only a gradual spin crossover was observed for both complexes, the transition temperature was shifted to higher temperatures relative to that of the complexes with no additional hydroxy groups at the Schiff base like ligand. The hydrogen-bonding network was responsible for this effect.

(© Wiley-VCH Verlag GmbH & Co. KGaA, 69451 Weinheim, Germany, 2009)

Introduction

The bistability of spin-transition complexes (spin crossover, SCO) is one of the most promising for new electronic devices in molecular memories and switches, as it may be controlled by different physical perturbations as temperature, pressure or light.^[1,2] Recent research activities in this field explore the possibility to combine this SCO bistability with additional properties (e.g., liquid crystalline properties,^[3] magnetic exchange interactions^[4]), resulting in multifunctional SCO materials;^[5] other research is based on the rational design of nanostructured SCO materials and their chemical and physical properties.^[6] Of the possible types of spin transitions (gradual, abrupt, with hysteresis, step wise, incomplete), much of the interest is focused on the bistability in highly cooperative systems (hysteresis or memory effect), and as such, compounds can exist in two different electronic states depending on the history of the system. With regard to this, we recently characterised an iron(II) spin-crossover complex with a 70 K wide thermal hysteresis loop around room temperature on the basis of a 2D network of hydrogen bonds between the complex molecules.^[7] Systematic investigations on the magnetic properties of iron(II) complexes of this ligand system demonstrated that hydrogen bonds are also the foundation for long-range

magnetic ordering.^[8] As a consequence of this finding, we designed a new ligand based on 4,5-diaminocatechol with two additional hydroxy groups on the phenyl ring that can act as H-bond donors/acceptors. In Scheme 1 the general procedure for the synthesis of the new ligand and the used abbreviations is given. In this paper we present the synthesis and characterisation of two octahedral iron(II) spin-crossover complexes of H_2L1 with pyridine (py) and *N,N'*-dimethylaminopyridine (dmap) as axial ligands. Special attention was given to the influence of the two additional hy-



[a] Center for Integrated Protein Science Munich at the Department Chemie und Biochemie, Ludwig-Maximilians-Universität München, Butenandtstr. 5-13 (Haus F), 81377 München, Germany
 Fax: +49-89-2180-77407
 E-mail: bwmch@cup.uni-muenchen.de

Scheme 1. General procedure for the synthesis of the new ligand H_2L1 and structures of the mononuclear complex $[FeL1]$, $[FeL2]$ and the axial ligands with the used abbreviations.

droxy groups on the spin-crossover properties. For this purpose, the properties of the two newly prepared complexes are compared with the previously published analogue complexes $[\text{FeL}2(\text{py})_2]$ and $[\text{FeL}2(\text{dmap})_2]$ with no additional hydroxy groups on the phenylene ring.^[9] Those two complexes both show a cooperative spin transition with an approximate 9 K-wide thermal hysteresis loop in the case of the dmap adduct ($T_{1/2} = 179$ K) and an approximate 2 K-wide thermal hysteresis loop in the case of the py adduct ($T_{1/2} = 190$ K). In both cases, the hysteresis is due to elastic interactions with several short van der Waals contacts, which are more pronounced in the case of the dmap adduct.^[9]

Results and Discussion

Synthesis and General Characterisation

In Scheme 1 the general structure of the mononuclear iron complexes $[\text{FeL}1/2]$ and the used axial ligands is given. Starting point for the synthesis of the new ligand $\text{H}_2\text{L}1$ is 4,5-diaminocatechol, which was prepared as described previously by Rosa et al.^[10] starting with commercially available veratrol. Condensation with two equivalents of the keto-enol ether (compound A^[11]) resulted in the formation of the desired ligand, which was characterised by elemental analysis and IR, mass and NMR spectroscopy. Conversion of the ligand with iron(II) acetate (1.3 equiv.) in methanol gave the iron(II) complex $[\text{FeL}1(\text{MeOH})]$. The desired octahedral complexes $[\text{FeL}1(\text{py})_2] \cdot \text{py}$ (**1**) and $[\text{FeL}1(\text{dmap})_2] \cdot \text{MeOH} \cdot 0.5\text{dmap}$ (**2**) were obtained by reaction of $[\text{FeL}1]$ with pyridine or dmap followed by slow crystallisation. Both complexes were fully characterised by elemental analysis and mass spectroscopy as well as temperature-dependent magnetic susceptibility measurements, X-ray structure analysis and temperature-dependent ^1H NMR spectroscopy in the case of **1**.

Description of the X-ray Structures

Crystals suitable for X-ray structure analysis were obtained for the two octahedral complexes. The crystallographic data are summarised in Table 5. The quality of the data of **2** was inferior and problems occurred with the refinement of the strongly disordered dmap and methanol solvent molecules. Therefore, those atoms were not refined anisotropically. We will only be publishing the conformation of the complex and the crystallographic data. In Fig-

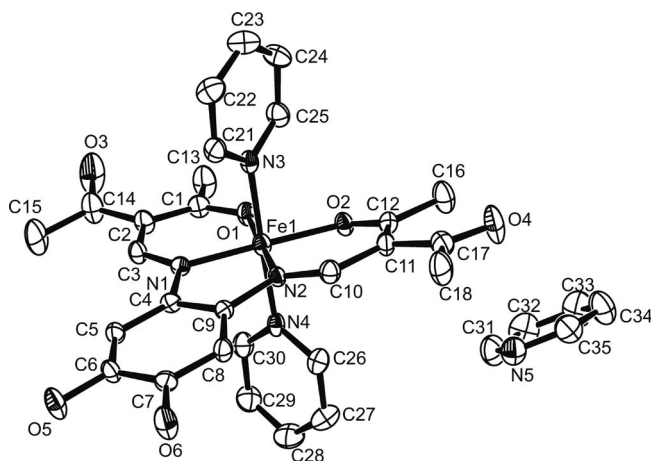


Figure 1. ORTEP drawing of the asymmetric unit of **1** with the atom numbering scheme. Hydrogen atoms are omitted for clarity. Thermal ellipsoids are shown at the 50% probability level.

ures 1 and 2 the asymmetric units of the two complexes are displayed. Selected bond lengths and angles within the first coordination sphere are summarised in Table 1.

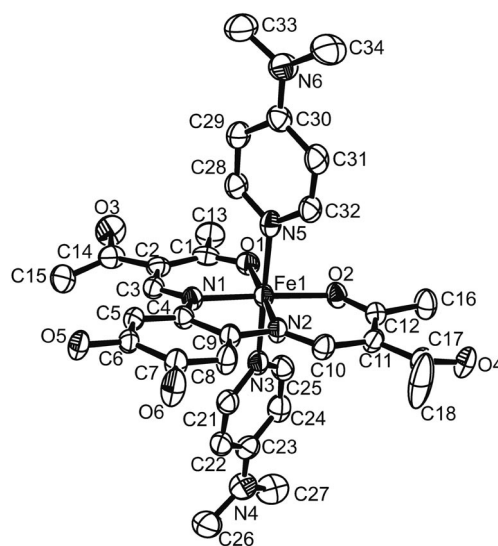


Figure 2. ORTEP drawing of the asymmetric unit of **2** with the atom numbering scheme. Hydrogen atoms and additional solvent molecules are omitted for clarity. Thermal ellipsoids are shown at the 50% probability level.

In both complexes, the iron centre is located in a distorted octahedral coordination sphere with a N_4O_2 surrounding. The bond lengths and angles within the first coordination sphere are within the region reported for low-spin (LS) iron(II) complexes of the same ligand type.^[12] The average bond lengths are 1.90 (Fe– N_{eq}), 1.94 (Fe– O_{eq}) and

Table 1. Selected bond lengths [\AA] and angles [$^\circ$] within the first coordination spheres of the complexes discussed in this work.

	Fe– N_{eq}	Fe– O_{eq}	Fe– N_{ax}	O1–Fe–O2	$\text{L}_{\text{ax}}\text{–Fe–L}_{\text{ax}}$
1	1.885(2), 1.899(2)	1.928(2), 1.929(1)	1.991(2), 1.996(2)	87.51(6)	178.49(7)
2	1.910(4), 1.912(3)	1.934(3), 1.952(3)	2.017(4), 2.032(4)	91.01(12)	176.25(15)

2.01 Å (Fe–N_{ax}). A characteristic tool for the determination of the spin state of these types of iron(II) complexes is the O–Fe–O angle, which changes from about 110° in the high-spin (HS) state to about 90° in the LS state.^[13] For the complexes reported here, the angle is 89°, which is clearly in the region typical for the LS state. The bond lengths observed for **2** are all slightly longer than the bond lengths of **1**, indicating an already started spin transition with a small fraction of HS molecules. The bond lengths within the FeOCCCN chelate six-membered ring of the equatorial ligand cannot be assigned to single and double bonds, indicating the delocalisation of the negative charge of the ligand over the chelating ring.

As already pointed out in the introduction, intermolecular interactions can play a crucial role for the obtained magnetic properties. They are not only relevant for cooperative interactions in spin-transition complexes^[7,13a,14,15] or long-range magnetic ordering,^[8,13b] as it is also known that H-bonds can influence the ligand field strength and by this the spin state of the iron complexes.^[16] In Table 2 selected intermolecular distances of **1** are summarised, and in Figure 3 the packing of the molecules of **1** in the crystal is displayed.

Table 2. Selected intermolecular distances [Å] and angles [°] of **1** resulting in a 1D chain with the base vector [0 1 0]. Only contacts shorter than the sum of the van der Waals radii –0.2 Å were considered.

	D–H	H...A	A...D	D–H...A
O5–H5...O4 ^[a]	0.82	1.81	2.627(2)	174.5
O6–H6...N5 ^[b]	0.82	1.95	2.693(3)	149.6
C26–H26...O6 ^[b]	0.93	2.46	3.163(3)	132.2
H25...H25 ^[c]		2.20		
H28...C6 ^[d]		2.57		
H23...H23 ^[e]		2.21		

[a] $x, 1 + y, z$. [b] $1 - x, -y, -z$. [c] $1 - x, -y, 1 - z$. [d] $1 + x, y, z$. [e] $-x, -y, 1 - z$.

The two hydroxy groups at the phenylene ring give rise to a 1D chain of H-bond-linked molecules along the base vector [0 1 0]. Both OH groups act as H-bond donors. One of the two donor contacts (H5) links directly two complex molecules over the OMe group (O4) of the neighbouring molecule. The second OH group (H6) forms a hydrogen bond to the nitrogen (N5) atom of the additional pyridine molecule included in the crystal packing and does not participate in the 1D chain of linked molecules. This chain, however, is further supported by a weak hydrogen bond between the aromatic CH hydrogen atom of a coordinated pyridine molecule (H26), involving the second hydroxy group as a H-bond acceptor (O6) and three further short van der Waals contacts (Table 2). In the case of **2**, a complete analysis of the intermolecular interactions is precluded because of the low quality of the X-ray structure and the strong disorder of the included solvent molecules. Only hydrogen bonds directly linking two complex molecules were considered. In Table 3 selected intermolecular distances are summarised, and in Figure 4 an excerpt of the packing of the molecules of **2** in the crystal is given. The

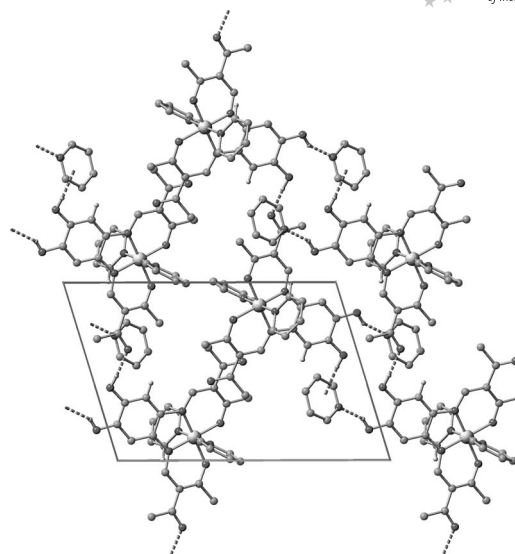


Figure 3. Packing of the molecules of **1** in the crystal. Hydrogen atoms not involved in the H-bonding network are omitted for clarity.

two hydroxy groups of the phenylene ring are involved as H-bond donors in two hydrogen bonds, both linking two complex molecules. One of the two donor contacts (H5A) links the molecules over the OMe group (O4) of the neighbouring complex in a similar fashion as that observed for

Table 3. Selected intermolecular distances [Å] and angles [°] of **2**.

	D–H	H...A	A...D	D–H...A
O5–H5A...O4 ^[a]	0.82	1.77	2.58	169
O6–H6...O5 ^[b]	0.82	2.02	2.71	143
C5–H5...O4 ^[b]	0.93	2.58	3.22	127

[a] $1/2 + x, 1/2 - y, 1/2 + z$. [b] $1 - x, 1 - y, 1 - z$.

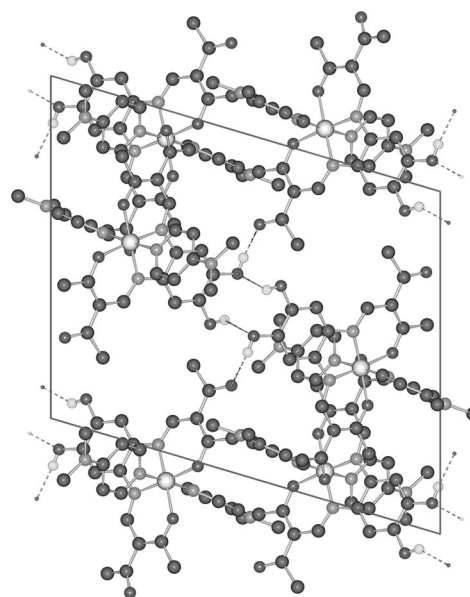


Figure 4. Packing of the molecules of **2** in the crystal. Hydrogen atoms not involved in the H-bonding network and additional solvent molecules are omitted for clarity.

1. The second OH group (H6) forms a hydrogen bond to the oxygen (O5) atom of the hydroxy group of a neighbouring molecule. Those two hydrogen bonds give rise to a 2D network of linked complex molecules along the plane (1 0 -1).

Magnetic Susceptibility Data

Magnetic susceptibility measurements were performed in the temperature range from 350 to 10 K for both complexes by using a Quantum design MPMSR2-SQUID magnetometer. Figure 5 displays the thermal dependence of the $\chi_M T$ product (with χ_M being the molar susceptibility and T the temperature) at 0.05 T for both compounds. For complex **1**, the room-temperature value is with $0.22 \text{ cm}^3 \text{ K/mol}$ in the region expected for a complex essentially in the LS state. Upon cooling, the value decreases further to $0.03 \text{ cm}^3 \text{ K/mol}$ at 100 K – a value typical for diamagnetic iron(II) complexes. Upon heating the complex above room temperature, the $\chi_M T$ product increases rapidly and reaches a value of $1.24 \text{ cm}^3 \text{ K/mol}$ at 350 K. This increase in the magnetic moment can be associated with a spin transition of the complex above room temperature that is still not complete at 350 K. The system was not heated any further to avoid loss of the pyridine molecules included in the crystal packing.

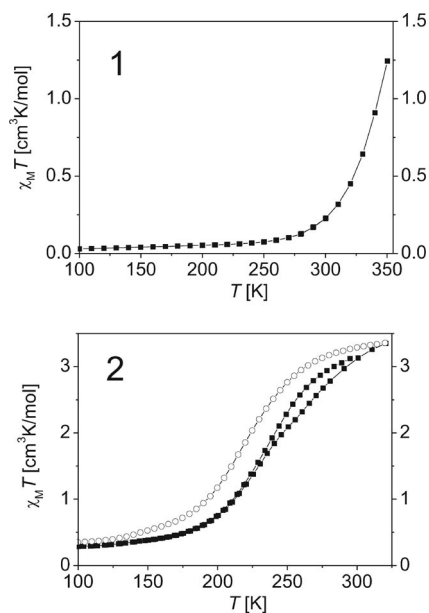


Figure 5. Plots of $\chi_M T$ product (filled squares) vs. T for compounds **1** (top) and **2** (bottom) at 0.05 T. The open circles correspond to the temperature dependence of the $\chi_M T$ product of **2** after heating to 320 K.

In the case of **2**, the room-temperature value of the $\chi_M T$ product is $3.12 \text{ cm}^3 \text{ K/mol}$, which is in the region expected for an iron(II) complex essentially in the HS state. Upon cooling, the magnetic moment decreases gradually and reaches a value of $0.29 \text{ cm}^3 \text{ K/mol}$ at 100 K. Compound **2**

undergoes a gradual spin transition with $T_{1/2} = 229 \text{ K}$. Upon heating, the transition curve differs slightly from the cooling curve and a small hysteresis is observed in the high-temperature region ($T_{1/2} = 231 \text{ K}$). Further heating of the complex to 320 K leads to a further increase in the $\chi_M T$ product to a value of $3.35 \text{ cm}^3 \text{ K/mol}$ expected for an iron(II) complex in the HS state. In the second cooling cycle, the transition temperature is shifted to lower temperatures ($T_{1/2} = 212 \text{ K}$) and this curve progression is obtained for all further heating and cooling cycles. The observed behaviour can be explained with a (partial) loss of the methanol molecules included in the crystal packing in the first heating cycle. A good agreement is obtained between the outcomes from the magnetic measurements and the results from X-ray crystallography. In contrast to the two parent compounds $[\text{FeL2}(\text{py})_2]$ and $[\text{FeL2}(\text{dmap})_2]$ with no additional hydroxy groups on the phenylene ring, no cooperative spin transition was obtained for **1** and **2**. The reason is most likely the inclusion of solvent molecules in the crystal packing, which reduces the number of direct short van der Waals contacts between the complex molecules. However, a positive effect of the introduced hydroxy groups is a shift in the transition temperature of the complexes to higher temperatures, and this temperature is in a region that is closer to room temperature.

^1H NMR Spectroscopy

We recently reported the possibility to follow a spin transition in solution by interpretation of the temperature dependence of the ^1H NMR chemical shifts of the compounds.^[17] In order to investigate the influence of the additional hydroxy groups on the spin transition in more detail, **1** was dissolved in a mixture of $[\text{D}_5]\text{pyridine}/[\text{D}_8]\text{toluene}$ (50:50). The iron centre was assumed to retain its octahedral coordination sphere; however, all hydrogen bonds observed in the crystal packing and any additional intermolecular interactions were disabled. This allowed us to evaluate the influence of packing effects on the transition curve of **1**. Figure 6 shows the ^1H NMR spectrum of **1** at 65°C with the signal assignment to the right. The assignment was accomplished by spectral comparison with previously published spectra^[17] and by taking the different line widths and relative intensities into consideration. The position of the signals of protons A, B and C with the relative intensities of 3 (A and B) and 1 (C) is comparable to those of the previously published complex $[\text{FeL2}(\text{py})_2]$ in a pyridine/toluene mixture (50:50). The signals were therefore assigned to the CH_3 groups (A, B) of the substituents of the equatorial ligand. The signal with a relative intensity of 1 was assigned to proton C of the phenylene ring. Of the two remaining protons, the signal of the OH proton D is observed in the 9 ppm region of the spectrum. The signal of the last proton was not assigned. Considering the NMR spectra of these types of complexes in pyridine,^[17] the HC-N proton should be in the 400–500 ppm region of the spectrum but is very broad and therefore difficult to detect.

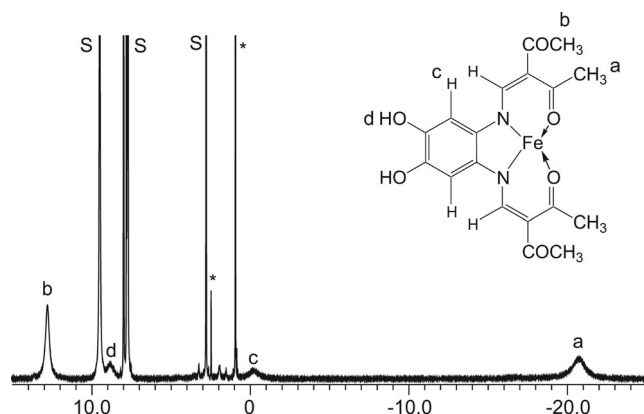


Figure 6. ¹H NMR spectrum of **1** in a [D₅]pyridine/[D₈]toluene (50:50) at 65 °C. The signal assignment is given at the right. S denotes the solvent toluene/pyridine and * denotes the impurities.

The temperature dependence of the NMR parameters of **1** (isotropic shifts plotted vs. $1/T$) is given in Figure 7 (top). Above 15 °C (288.15 K; $1/T = 3.5 \text{ 1000/K}$) the behaviour is similar to those expected for pure HS complexes. At lower temperatures, the isotropic shifts move rapidly towards zero as reported previously for these types of spin-transition complexes.^[17] The paramagnetic shift of the pure HS complex above 15 °C does not follow the ideal Curie law straight line. This is most probably due to thermally accessible excited states. The experimental data in Figure 7 (top)

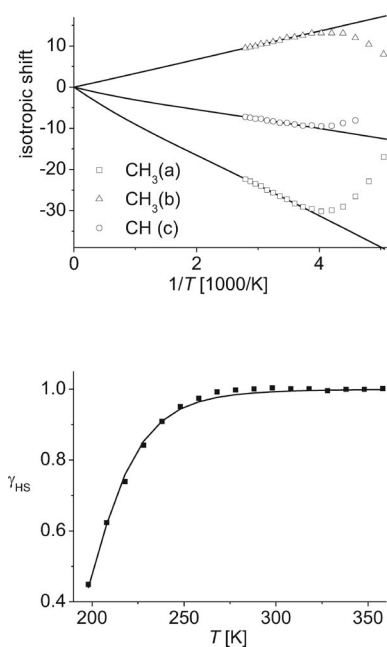


Figure 7. Top: Isotropic shifts of **1** plotted vs. $1/T$ (dots). The solid lines represent the calculated shifts of the pure HS complex by using the extended Curie law [Equation (1)]. The fitting parameters are given in the text. Bottom: HS mol fraction (γ_{HS}) of **1** obtained by interpretation of the isotropic shifts by using the extended Curie law. The solid line corresponds to fitted data by using the regular solution model with the parameters given in the text.

were fit by taking an extended Curie law into account with different Curie constants (or spin densities) for the ground and excited states:

$$\delta_n^{\text{con}} = (F/T)\{W_1 C_{n1}^2 = +W_2 C_{n2}^2 e^{-\Delta E/kT}\} / \{W_1 + W_2 e^{-\Delta E/kT}\} \quad (1)$$

where W_1 and W_2 are the weighting factors for the ground and excited states [$S(S+1)$ in each case], C_{n1} and C_{n2} are the orbital coefficients (spin densities) for the ground state and excited state, F is the Curie constant, ΔE is the energy difference between the ground state and the first excited state and k is the Boltzmann constant. Because the most likely excited state is that in which the formerly t_{2g} electrons are rearranged between the d_{xy} and d_{yz} orbitals, both the ground state and the first excited state were assumed to exhibit a total spin $S = 2$. Other possible spin states were also tried but produced no reliable fits. The fit obtained with the TDF (temperature-dependent fitting) program written by Shokhirev and Walker^[18] (solid lines) simulates the temperature dependence of the isotropic shift very well. The best-fit parameters are: $E_1(\text{GS}) = 2 [(d_{xy})^2 - (d_{xz}, d_{yz})^2] (d_{z^2})^1 (d_{x^2-y^2})^1$, $E_1(\text{ES}) = 2 [(d_{xy})^1 (d_{xz}, d_{yz})^3 (d_{z^2})^1 (d_{x^2-y^2})^1]$, $\Delta E_{1,2} = 744 \text{ cm}^{-1}$, MSD (mean standard deviation) = 0.073, spin densities 1: $-0.013(\text{a}), 0.006(\text{b}), 0.005(\text{c})$; 2: $-0.022(\text{a}), 0.005(\text{b}), 0.001(\text{c})$. The calculated isotropic shifts of the pure HS complex at lower temperature can now be used to determine the HS molar fraction (γ_{HS}) of the complex as a function of temperature:

$$\gamma_{\text{HS}} = [\delta^{\text{con}}(\text{measured})T] / [\delta^{\text{con}}(\text{calculated})T] \quad (2)$$

In Figure 7 (bottom), the average of the spin transition curves for the different protons is given (dots). The data were fitted using the expression:

$$-RT \ln[\gamma_{\text{HS}} / (1 - \gamma_{\text{HS}})] = \Delta H_{\text{HL}} - T \Delta S_{\text{HL}} \quad (3)$$

where ΔH_{HL} and ΔS_{HL} are the thermodynamic enthalpy and entropy values associated with the spin transition (solid line). The obtained fitting parameters are $\Delta H_{\text{HL}} = 25.1 \pm 1.1 \text{ kJ/mol}$ and $\Delta S_{\text{HL}} = 124.5 \pm 5.3 \text{ J/K mol}$ with a transition temperature of $T_{1/2} = 201 \text{ K}$. The obtained entropy change is quite high (about three times the expected value), indicating that either cooperative interactions are not totally negligible or there are some dynamics in the compound. The transition temperature obtained in solution is significantly lower than the transition temperature in the solid state and the solid-state properties are clearly influenced by the crystal packing.

Conclusions

Two new spin-crossover complexes were prepared with an N₂O₂ coordinating Schiff base like ligand that was altered by introduction of two additional hydroxy groups with the idea to provide better preconditions for the formation of a hydrogen-bonding network. The aim of this modification was to synthesise more examples of H-bond-linked spin-crossover complexes similar to our previous complex with a 70 K-wide thermal hysteresis loop^[7] to provide a bet-

ter understanding about the suitability of hydrogen bonds to transmit cooperative interactions during the spin transition. In this work, we present that the new modification was only partly successful. The outcomes from X-ray structure analysis clearly demonstrate that, as requested, the introduced hydroxy groups give rise to the formation of a network of H-bond-linked molecules. However, in contrast to the two parent compounds [FeL2(py)₂] and [FeL2(dmap)₂] additional solvent molecules are included in the crystal packing. As a consequence, only gradual spin transitions are observed for these two complexes. In order to investigate the influence of the H-bonding network on cooperative interactions during the spin transition, it will be necessary to prepare complexes with no included solvent molecules.

However, comparative studies in solution and in the solid state clearly demonstrate an effect of the H-bonding network on the transition temperature, as summarised in Table 4. In solution, the effect of the introduction of a hydroxy group on the phenylene ring of the Schiff base like ligand is marginal, and nearly the same transition temperatures are obtained for complexes **1** and [FeL2(py)₂]. In contrast to this, a difference of about 150 K is obtained for the transition temperatures in the solid state and the only possible reason is the observed H-bonding network in the case of **1**. Systematic investigations on about 20 octahedral mononuclear iron(II) complexes of this ligand system with N-heterocycles as axial ligands revealed a systematic effect of the substituents at the Schiff base like ligand on the overall ligand field strength.^[13] Substituents with a negative mesomeric effect [(–)-M] at the OCCCN chelating six-membered ring of the ligand lead to a reduction in the electron density at the donor atoms and a reduced ligand field strength.^[13] In the crystal packing of **1** and **2** a hydrogen bond between the OH group and the COMe substituent at the chelating six-membered ring is observed. However, this hydrogen bond should increase the (–)-M effect of this substituent and thus lead to a reduction in the ligand field strength. A more likely explanation is that due to the hydrogen bonds, the electron density at the hydroxy oxygen atom is increased to such an extent that instead of a negative inductive [(–)-I] and a (+)-M effect of an OH group, a (+)-I and a (+)-M effect is observed, similar to an O[–] substituent. This results in an increase in the electron density at the nitrogen donor atom in the *para*-position and an increase in the overall ligand field strength. Thus, the spin transition is shifted to higher temperatures. In the case of complex **2**, one hydrogen bond

involves the OH group of the neighbouring molecule as a H-bond acceptor. This probably compensates the effects described above and the influence of the H-bond network on the ligand field strength is less pronounced compared to that in **1**, in agreement with the outcome of the magnetic measurements.

Experimental Section

Synthesis: All syntheses were carried out under an atmosphere of argon by using Schlenk tube techniques. All solvents were purified as described in the literature^[19] and distilled under an atmosphere of argon. The synthesis of 4,5-diaminocatechol,^[10] compound A^[11] and iron(II)acetate^[20] is described in literature.

H₂L1: To a solution of 4,5-diaminocatechol dihydrobromide (4.60 g, 15.23 mmol) and sodium methoxide (1.66 g, 30.73 mmol) in methanol (120 mL) was added compound A (4.80 g, 30.73 mmol) in methanol (20 mL) in one portion. The solution was stirred for 16 h at room temperature. After this time the precipitate was filtered off, recrystallised from ethanol and dried in vacuo. Yield: 5.38 g (98%). C₁₈H₂₀N₂O₆ (360.36): calcd. C 59.99, H 5.59, N 7.77; found C 58.78, H 5.60, N 7.57. IR (nujol): $\tilde{\nu}$ = 1603 (C=O, COMe), 3101 (br., OH) cm^{–1}. MS (FAB+): *m/z* (%) = 361 (20) [H₂L1 + H]⁺. ¹H NMR (270 MHz, CDCl₃): δ = 2.25 (s, 6 H, CO-CH₃), 2.34 (s, 6 H, CO-CH₃), 6.94 (s, 2 H, CH-phenylene), 8.16 (d, 2 H, CH=C), 9.5 (s, 2 H, OH), 12.58 (d, 2 H, NH) ppm.

[FeL1(MeOH)]: A suspension of iron(II)acetate (3.05 g, 17.5 mmol) and H₂L1 (4.86 g, 13.51 mmol) in methanol (150 mL) was heated at reflux for 2 h. After cooling, a red brown precipitate was obtained that was collected, washed with methanol (2 × 20 mL) and dried in vacuo. Yield: 3.22 g (65%). C₁₉H₂₂FeN₂O₇ (446.23): calcd. C 51.14, H 4.97, N 6.28; found C 50.89, H 5.15, N 6.28. MS (DEI+): *m/z* (%) = 31 (100) [MeOH]⁺, 414 (5) [FeL1]⁺. IR (nujol): $\tilde{\nu}$ = 1606 (C=O, COMe), 3300 (br., OH) cm^{–1}.

[FeL1(py)₂](py) (1**):** A solution of [FeL1(MeOH)] (0.40 g, 0.89 mmol) in pyridine (15 mL) was heated at reflux for 30 min. After this time, oxygen-free water (15 mL) was added. Cooling the mixture to 4 °C yielded a fine crystalline black precipitate of **1** that was collected and dried in vacuo. Yield: 0.30 g (50%). C₃₃H₃₃FeN₅O₆ (651.49): calcd. C 60.84, H 5.11, N 10.75; found C 60.81, H 5.09, N 10.85. MS (FAB+): *m/z* (%) = 79 (100) [py]⁺, 414 (35) [FeL1]⁺. IR (nujol): $\tilde{\nu}$ = 1652 (C=O, COMe), 3070 (br. OH) cm^{–1}.

[FeL1(dmap)₂](MeOH)(dmap)_{0.5} (2**):** A solution of [FeL1(MeOH)] (0.50 g, 1.30 mmol) and dmap (6.35 g, 51.99 mmol) in methanol (90 mL) was heated at reflux for 1.5 h. Cooling the mixture to 4 °C yielded a fine crystalline black precipitate of **2** that was collected, washed with methanol (5 mL) and dried in vacuo. Yield: 0.30 g (33%). C_{36.5}H₄₈FeN₇O_{7.5} (760.66): calcd. C 57.63, H 6.36, N 12.89; found C 57.50, H 6.11, N 12.86. MS (FAB+): *m/z* (%) = 123 (100) [dmap], 413 (25) [FeL1]⁺. IR (nujol): $\tilde{\nu}$ = 1610 (C=O, COMe), 3444 (br., OH) cm^{–1}.

Magnetic Measurements: Magnetic measurements of the fine crystalline samples were performed with a Quantum-Design-MPMSR2-SQUID-Magnetometer in a temperature range from 10 to 350 K. The measurements were carried out at 0.05 T in the settle mode. The data were corrected for the magnetisation of the sample holder and diamagnetic corrections were made by using tabulated Pascal's constants.

Table 4. Comparison of the transition temperatures of the four complexes **1**, **2**, [FeL2(py)₂] and [FeL2(dmap)₂] discussed in this work in solution and in the solid state.

Complex	<i>T</i> _{1/2} [K], solid state	<i>T</i> _{1/2} [K], solution	Ref.
1	>350	201	this work
2	230		this work
[FeL2(py) ₂]	190	211	[5,13]
[FeL2(dmap) ₂]	179		[5]

X-ray Crystallography: The intensity data of **2** were collected with a Nonius KappaCCD diffractometer by using graphite-monochromated Mo-*K*_α radiation. The intensity data of **1** were collected with an Oxford XCalibur diffractometer by using graphite-monochromated Mo-*K*_α radiation. Data were corrected for Lorentz and polarisation effects. The structure was solved by direct methods (SIR97^[21]) and refined by full-matrix least-square techniques against *F*_o² (SHELXL-97^[22]). The hydrogen atoms were included at calculated positions with fixed thermal parameters. ORTEP-III was used for structure representation.^[23] Crystallographic data are summarised in Table 5. Selected distances and angles are presented in Table 1. CCDC-744753 (for **1**) and -744754 (for **2**) contain the supplementary crystallographic data for this paper. These data can be obtained free of charge from The Cambridge Crystallographic Data Centre via www.ccdc.cam.ac.uk/data_request/cif.

Table 5. Crystallographic data of the octahedral complexes discussed in this work.

	1	2
Empirical formula	C ₃₃ H ₃₃ FeN ₅ O ₆	C _{36.5} H ₄₈ FeN ₇ O _{7.5}
Formula weight	651.49	760.66
Temperature [K]	200	200
Crystal size [mm]	0.30 × 0.21 × 0.13	0.24 × 0.21 × 0.024
Crystal system	triclinic	monoclinic
Space group	<i>P</i> $\bar{1}$	<i>P</i> ₂ / <i>n</i>
<i>λ</i> [Å]	0.71073	0.71073
<i>a</i> [Å]	8.709(4)	16.2330(5)
<i>b</i> [Å]	11.767(3)	12.6390(4)
<i>c</i> [Å]	16.660(2)	19.2770(5)
<i>α</i> [°]	104.894(16)	90
<i>β</i> [°]	94.73(2)	106.548(2)
<i>γ</i> [°]	105.38(3)	90
<i>V</i> [Å ³]	1569.9(9)	3791.23(19)
<i>Z</i>	2	4
<i>ρ</i> _{calcd.} [g/cm ³]	1.378	1.3221
<i>μ</i> [1/mm]	0.533	0.455
<i>F</i> (000)	680	1584
<i>θ</i> range [°]	3.74–26.25	3.13–24.11
Index ranges	–10/10 –14/14 –20/20	–18/18 –14/14 –22/22
Reflections collected	25475	20985
Reflections unique	6388	6008
Data/restraints/parameters	6388/0/415	6008/0/476
<i>R</i> ₁ (all)	0.0347 (0.0686)	0.0525 (0.0706)
<i>wR</i> ₂	0.0701 (0.0791)	0.1392 (0.1510)
Goof	0.931	1.029

Acknowledgments

This work has been supported financially by the Deutsche Forschungsgemeinschaft (SPP 1137) the Fonds der Chemischen Industrie, the Center for Integrated Protein Science Munich (CIPSM) and the University of Munich. The authors thank P. Mayer for acquisition of the crystallographic data of **2**.

[1] a) P. Gütllich, A. Hauser, H. Spiering, *Angew. Chem. Int. Ed. Engl.* **1994**, *33*, 2024, and references cited therein; b) P. Gütllich, H. A. Goodwin (Eds.), *Topics in Current Chemistry Vols. 233–235: Spin Crossover in Transition Metal Compounds I–III*, Springer, Berlin, **2004**; c) J. A. Real, A. B. Gaspar, M. C. Muñoz, *Dalton Trans.* **2005**, 2062; d) M. Sorai, M. Nakano, Y.

- Miyazaki, *Chem. Rev.* **2006**, *106*, 976; e) A. B. Gaspar, M. C. Muñoz, J. A. Real, *J. Mater. Chem.* **2006**, *16*, 2522; f) O. Sato, J. Tao, Y.-Z. Zhang, *Angew. Chem.* **2007**, *119*, 2200; *Angew. Chem. Int. Ed.* **2007**, *46*, 2152–2187; g) S. Brooker, J. A. Kitchen, *Dalton Trans.* **2009**, 7331–7340.
- [2] a) O. Kahn, C. Jay Martinez, *Science* **1998**, *279*, 44–48; b) O. Kahn, C. Jay, J. Kröber, R. Claude, F. Grolrière, Patent **1995** EP0666561; c) J.-F. Létard, O. Nguyen, N. Daro, Patent **2005** FR0512476; d) J.-F. Létard, P. Guionneau, L. Goux-Capes in *Topics in Current Chemistry* (Eds.: P. Gütllich, H. A. Goodwin), Springer, Berlin, **2004**, vol. 235, p. 221; e) A. Galet, A. B. Gaspar, M. C. Muñoz, G. V. Bukin, G. Levchenko, J. A. Real, *Adv. Mater.* **2005**, *17*, 2949–2953.
- [3] a) M. Seredyuk, A. B. Gaspar, V. Ksenofontov, Y. Galyametdinov, M. Verdager, F. Villain, P. Gütllich, *Inorg. Chem.* **2008**, *47*, 10232–10245; b) M. Seredyuk, A. B. Gaspar, V. Ksenofontov, Y. Galyametdinov, J. Kusz, P. Gütllich, *Adv. Funct. Mater.* **2008**, *18*, 2089; c) M. Seredyuk, A. B. Gaspar, V. Ksenofontov, Y. Galyametdinov, J. Kusz, P. Gütllich, *J. Am. Chem. Soc.* **2008**, *130*, 1431.
- [4] a) J. A. Real, A. B. Gaspar, V. Niel, M. C. Muñoz, *Coord. Chem. Rev.* **2003**, *236*, 121; b) A. Bousseksou, G. Molnár, J. A. Real, K. Tanaka, *Coord. Chem. Rev.* **2007**, *251*, 1822–1833.
- [5] a) A. B. Gaspar, V. Ksenofontov, M. Seredyuk, P. Gütllich, *Coord. Chem. Rev.* **2005**, *249*, 2661–2676; b) A. B. Gaspar, M. Seredyuk, P. Gütllich, *J. Mol. Struct.* **2009**, *924–926*, 9–19.
- [6] a) I. Boldog, A. B. Gaspar, V. Martinez, P. Pardo-Ibanez, V. Ksenofontov, A. Bhattacharjee, P. Gütllich, J. A. Real, *Angew. Chem. Int. Ed.* **2008**, *47*, 6433–6437; b) S. Cobo, G. Molnár, J. A. Real, A. Bousseksou, *Angew. Chem. Int. Ed.* **2006**, *45*, 5786–5789; c) G. Molnár, S. Cobo, J. A. Real, F. Carcenac, E. Daran, C. Vien, A. Bousseksou, *Adv. Mater.* **2007**, *19*, 2163.
- [7] B. Weber, W. Bauer, J. Obel, *Angew. Chem.* **2008**, *120*, 10252–10255; *Angew. Chem. Int. Ed.* **2008**, *47*, 10098–10101.
- [8] a) B. R. Müller, G. Leibeling, E.-G. Jäger, *Chem. Phys. Lett.* **2000**, *319*, 368–374; b) B. Weber, E.-G. Jäger, *Z. Anorg. Allg. Chem.* **2009**, *635*, 130–133.
- [9] B. Weber, E. Kaps, J. Weigand, C. Carbonera, J.-F. Létard, K. Achterhold, F.-G. Parak, *Inorg. Chem.* **2008**, *47*, 487–496.
- [10] D. T. Rosa, R. A. Reynolds, S. M. Malinak, D. Coucouvanis, *Inorg. Synth.* **2002**, *33*, 112–119.
- [11] L. Claisen, *Justus Liebigs Ann. Chem.* **1897**, *279*, 1.
- [12] a) B. Weber, E. S. Kaps, J. Obel, W. Bauer, *Z. Anorg. Allg. Chem.* **2008**, 1421–1426; b) B. Weber, C. Carbonera, C. Desplanches, J.-F. Létard, *Eur. J. Inorg. Chem.* **2008**, 1589–1598; c) B. Weber, E. S. Kaps, C. Desplanches, J.-F. Létard, K. Achterhold, F.-G. Parak, *Eur. J. Inorg. Chem.* **2008**, 4891–4898; d) W. Bauer, B. Weber, *Inorg. Chim. Acta* **2009**, *362*, 2341–2346; e) B. Weber, E. Kaps, *Heteroat. Chem.* **2005**, *16*, 391–397; f) B. Weber, E. S. Kaps, J. Obel, K. Achterhold, F. G. Parak, *Inorg. Chem.* **2008**, *47*, 10779–10787; g) B. Weber, R. Tandon, D. Himsl, *Z. Anorg. Allg. Chem.* **2007**, *633*, 1159–1162; h) B. Weber, E. S. Kaps, C. Desplanches, J.-F. Létard, *Eur. J. Inorg. Chem.* **2008**, 2963–2966.
- [13] a) B. Weber, *Coord. Chem. Rev.* **2009**, *253*, 2432–2449; b) B. Weber, E.-G. Jäger, *Eur. J. Inorg. Chem.* **2009**, 465–477.
- [14] J. A. Real, A. B. Gaspar, V. Niel, M. C. Muñoz, *Coord. Chem. Rev.* **2003**, *236*, 121–141.
- [15] N. Bréfuel, S. Imatomi, H. Torigoe, H. Hagiwara, S. Shova, J.-F. Meunier, S. Bonhommeau, J.-P. Tuchagues, N. Matsumoto, *Inorg. Chem.* **2006**, *45*, 8126–8135.
- [16] A. P. Summerton, A. A. Diamantis, M. R. Snow, *Inorg. Chim. Acta* **1978**, *27*, 123–128.
- [17] B. Weber, F. A. Walker, *Inorg. Chem.* **2007**, *46*, 6794–6803.
- [18] N. V. Shokhirev, F. A. Walker, “Temperature-Dependent Fitting” <http://www.shokhirev.com/nikolai/abc/tdf/tdf4.html>.
- [19] Autorenkollektiv: *Organikum*, Johann Ambrosius Barth Verlagsgesellschaft mbH **1993**.
- [20] B. Heyn, B. Hipler, G. Kreisel, H. Schreer, D. Walter, *Anorganische Synthesechemie*, 2. Auflage, Springer, Heidelberg, **1986**.

- [21] *SIR97*, Campus Universitario Bari, **1997**: A. Altomare, M. C. Burla, G. M. Camalli, G. Cascarano, C. Giacovazzo, A. Guagliardi, A. G. G. Moliterni, G. Polidori, R. Spagna, *J. Appl. Crystallogr.* **1999**, *32*, 115.
- [22] G. M. Sheldrick, *SHELXL-97*, University of Göttingen, Germany, **1993**.
- [23] C. K. Johnson, M. N. Burnett, *ORTEP-III*, Oak-Ridge National Laboratory, Oak-Ridge, **1996**; L. J. Farrugia, *J. Appl. Crystallogr.* **1997**, *30*, 565.

Received: August 27, 2009

Published Online: November 4, 2009